

X-ray standing-wave study of alkali-metal/Si(111)7×7 interfaces

V. Eteläniemi,* E.G. Michel,[†] and G. Materlik

Hamburger Synchrotronstrahlungslabor (HASYLAB) at Deutsches Elektronen-Synchrotron (DESY), Notkestrasse 85, D-22603 Hamburg, Federal Republic of Germany

(Received 10 February 1993; revised manuscript received 13 July 1993)

The x-ray standing-wave technique was applied to study the interfaces formed between alkali metals (Rb, Cs) and Si(111)7×7. Through the use of two Bragg reflections [(111) and (220)], the distance of the adsorbate atoms to two bulk lattice planes was measured, which facilitated the determination of the adsorption site for different adsorbate coverages and annealing temperatures. Both alkali metals behaved in a similar way. At room-temperature saturation coverage, a rather disordered adsorption was observed, having at least on-top and threefold-hollow sites (normal and eclipsed). After an anneal of the adlayer and coverage reduction, the occupation of hollow sites of normal type was promoted. At very low coverages ($\Theta < 0.1$ monolayer) a significant increase in the distance from alkali-metal atoms to the bulklike surface was detected for both Rb and Cs. The increase is attributed to occupation of on-top sites in this coverage range. The reasons for this behavior are discussed on the basis of different models for the interface.

I. INTRODUCTION

In recent years there has been a large research effort devoted towards understanding the electronic and geometric structure of alkali-metal/silicon interfaces, from both the experimental and the theoretical points of view.^{1,2} The interest in these systems has increased partly due to the fact that they are considered especially simple cases of metal/semiconductor interfaces, since no chemical reactions or interdiffusion between metal and semiconductor take place at these surfaces.¹ In addition, the electronic structure of alkali metals is also very simple. These facts make alkali-metal/silicon interfaces true model systems for studying topics such as Schottky barrier formation, metallization, etc.³ In spite of these efforts, and the large amount of experimental information collected, the determination of the adsorption site of alkali metals has received less attention than other topics. Detailed knowledge of the adsorption site and its possible dependence on coverage, surface ordering, etc. is of high importance whenever theoretical and experimental results are to be compared.⁴ In particular, the adsorption site of the alkali-metal/Si(111)7×7 interface has been directly studied only very recently, although indirect information on the surface geometric structure was previously obtained by several groups. Daimon and Ino⁵ and Mizuno and Ichimiya⁶ have proposed adsorption on top of the adatoms of the Si(111)7×7 surface. Photoemission results⁷⁻⁹ suggested the presence of two types of sites in the case of Cs. Recent scanning tunneling microscopy (STM) results by Hashizume and co-workers^{10,11} have shown a more complex behavior: at low coverage, the authors have proposed adsorption on top of the adatoms, but at higher coverages trimers of Cs atoms were observed. At even higher coverages, patches of 1×3 symmetry appeared, and in this case a threefold (3F)-hollow site

of normal type (site *B*, see Fig. 1) was predominant. The 1×3 phase was observed by Daimon and Ino,⁵ and was studied later on by Fan and Ignatiev.¹² Tikhov, Surnev, and Kiskinova¹³ and Jeon *et al.*¹⁴ studied the reconstruction in the case of Na/Si(111)7×7. Very recently, the x-ray standing-wave (XSW) technique has been also applied to these systems.^{15,16} Concerning theoretical work, Northrup,¹⁷ Batra and Ciraci,¹⁸ Ossicini, Areangeli, and Bisi,¹⁹ Huaxiang and Ling,²⁰ and Moullet, Andreoni, and Parrinello²¹ have favored hollow sites (see Fig. 1 and Secs. IV and V) for adsorption of alkali metals on the Si(111)1×1 surface.

In a previous work¹⁵ we have presented XSW results for Cs/Si(111)7×7. The conclusion was that at room-temperature saturation coverage a mixture of sites is present. A mild annealing increased the ordering of the adsorbate and the occupation of hollow sites of normal type. Further annealing (and coverage reduction) produced an increase in the distance from Cs atoms to the Si surface, which was interpreted as being due either to a coverage-dependent bond-length change, or to occupation of a new site. We could not unequivocally discriminate between these two possibilities. In this paper we will give full account of our results for Cs/Si(111)7×7, and will present an analogous study for Rb/Si(111)7×7.

II. EXPERIMENT

The experiments were done using the synchrotron light from the DORIS storage ring at Hamburg Synchrotronstrahlungslabor (HASYLAB), monochromatized by a nondispersive double-crystal setup. The experimental system, consisting of three permanently mounted ultra-high vacuum (UHV) chambers (base pressure: 5×10^{-11} mbar), has been described in detail elsewhere.²² The cov-

erages (Θ) were determined from the ratio of the fluorescence intensities of the adsorbate ($L\alpha$ and $K\alpha$ lines, for Cs and Rb, respectively) and substrate ($K\alpha$ line) atoms. The accuracy of the cited coverages is better than 10%. All coverages are given in monolayers (ML) (1 ML = 7.8×10^{14} atoms/cm²), the atomic density of the bulk terminated Si(111) surface. In principle, a predetermined coverage can be obtained by annealing a saturated surface at a certain temperature for a fixed time. Since the temperatures employed are in the range of desorption temperatures, and the times were, in general, short, the reproducibility of a coverage is only approximate by this method. This fact explains why nominally identical annealing cycles can actually produce different coverages.

The samples were cut from a Si single-crystal block, mechanically polished, etched, and chemically cleaned using the procedure of Ishizaka and Shiraki²³ before insertion in the UHV chamber. Once in UHV, the samples were degassed for a long time at 600 °C, and finally annealed to 900 °C in a vacuum of better than 5×10^{-10}

mbar. After this preparation procedure, a sharp 7×7 low-energy electron-diffraction (LEED) pattern was observed, without significant traces of contamination as judged by Auger electron spectroscopy (AES).

The alkali metals Rb and Cs were evaporated from a commercial source (SAES-Getters, Italy). A Si(111) 7×7 surface [held at room temperature (RT)] was saturated with the alkali metal, and then annealed to increasingly higher temperatures. These annealing cycles made it possible both to improve the ordering of the adsorbate and to decrease the coverage. A freshly prepared surface was used for each annealing cycle. In some cases, Rb was directly deposited on a substrate held at elevated temperature. The accumulation times varied from 15 min to 5 h, depending on the alkali-metal coverage, the incident photon flux, and other experimental conditions. In the environment of the analysis chamber (where no pressure increases take place) the alkali-metal covered surfaces remained clean during the measurements, as judged by AES. The perfection of the substrate crystal (evaluated from the shape of the rocking curve and from three-crystal topography²⁴) was not significantly diminished by the annealing cycles. The sample crystals were slightly miscut in the case of Rb studies, with an asymmetry angle of 1.2° (i.e., the ratio of the direction cosines $|b| < 1$).

III. DATA ANALYSIS

We will give here a brief account of XSW data analysis, and refer the reader to Ref. 25 for a more detailed presentation. The XSW technique allows one to accurately measure the distance between the adsorbed atoms and a certain lattice plane. By measuring the distances to several lattice planes, the adsorption site can be determined. The process which takes place during a measurement can be summarized as follows: an incident x-ray wave is totally reflected by a single crystal in the angular range associated with the Bragg condition.²⁶ A standing-wave field is generated by constructive interference of incident and reflected waves. The nodes of the standing wave sweep over the atomic planes in the angular range of total reflection, producing a characteristic modulation in the induced fluorescence of both adsorbate and substrate. In XSW experiments two signals are simultaneously measured: the sample reflectivity R for a certain Bragg reflection and a signal coming from the atoms of interest, in our case fluorescence radiation. According to the dynamical theory of x-ray scattering, the normalized fluorescence yield $Y(\theta)$ of an adsorbate^{25,27} changes with the angle θ in the region of total reflection as

$$Y(\theta) = 1 + R(\theta) + 2\sqrt{R(\theta)}f_c \cos[2\pi(\nu(\theta) - \Phi)] \quad (1)$$

where $\nu(\theta)$ is the phase difference between reflected and incident wave and Φ , f_c (phase and coherent fraction) are two parameters. Φ is related to the positions of the adsorbate atoms of interest, and f_c to the fraction of atoms at these positions. When atoms are located coherently only at one type of adsorption site, f_c is, in fact, the

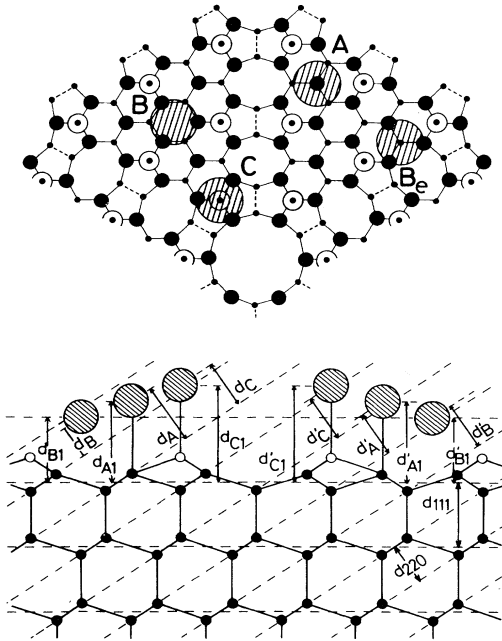


FIG. 1. Adsorption sites on the Si(111) 7×7 surface (atomic sizes not at scale; solid circles, Si atoms; open circles, last-layer Si atoms; hatched circles, alkali-metal atoms). Upper part, top view of the surface. Lower part, side view of the 7×7 reconstructed surface, with the unfaulted (left) and faulted (right) parts of the unit cell. Several high-symmetry sites have been considered: A (on top), B (threefold-hollow of normal type), B_e (threefold-hollow eclipsed, not shown in the side view), and C (adatom on top). Two distances used in this work for triangulation are shown: distance to the [111] plane (denoted in the side view as d_{A1} , d_{B1} , etc.), and distance to the [220] planes (denoted in the side view as d_A , d_B , etc.). Additionally, the presence of the stacking fault results in sites A and B having a different distance to the [220] plane for the faulted and unfaulted halves of the 7×7 unit cell. The distances corresponding to the faulted half are denoted with primed letters in the side view (e.g., d'_A , d'_{B1}).

percentage of atoms adsorbed at a distance Φ (in units of the lattice spacing), measured from the corresponding bulk diffracting plane. When the adsorption takes place at N types of adsorption sites (n coherent and the rest random) and fractions f_j ($\sum_{j=1}^N f_j = 1$) of the atoms are at distances Φ_j , it is not difficult to derive²⁵ that

$$\tan(2\pi\Phi) = \frac{\sum_j f_j \sin(2\pi\Phi_j)}{\sum_i f_i \cos(2\pi\Phi_i)}, \quad (2)$$

and

$$f_c^2 = \sum_j f_j^2 + 2 \sum_j \sum_{l < j} f_j f_l \cos[2\pi(\Phi_j - \Phi_l)], \quad (3)$$

where the summations are over the n coherent sites. Both f_c and Φ are obtained by fitting Eq. (1) to the experimental fluorescence yield. The adsorption sites can be identified in an XSW study by employing different Bragg reflections (which allows one to perform a triangulation), and/or by comparing the measured phase for one reflection with an expected phase, obtained from a certain adsorption model. In general, some information on the surface geometry and the bond length is very helpful for the analysis, although not strictly needed.

IV. RESULTS

We have carried out two independent sets of XSW measurements corresponding to the (111) and (220) substrate Bragg reflections. In each case, samples with different coverages and annealing temperatures were prepared. The [111] planes are parallel to the surface, and thus the adsorption distance normal to the surface is determined by a (111) measurement. The [220] planes make an angle of 35.3° to the surface. This reflection probes the lateral registration of the adsorbate atoms (see Fig. 1).

The results of the measurements for Rb/Si(111)7×7 (coherent phases Φ and fractions f_c) appear in Table I. The corresponding fluorescence yield curves are shown in Figs. 2–4, which include one rocking curve $R(\theta)$ in each case. We refer the reader to Ref. 15 for the (111) reflection results corresponding to Cs/Si(111)7×7. In the case of the (220) reflection and Cs/Si(111)7×7, we have measured one more coverage than in Ref. 15. We show here the whole set of (220) data in Fig. 5 and Table II for the sake of completion.

A very similar behavior was observed in both cases (Rb and Cs) from the point of view of the LEED patterns. After alkali-metal deposition at RT the 7×7 pat-

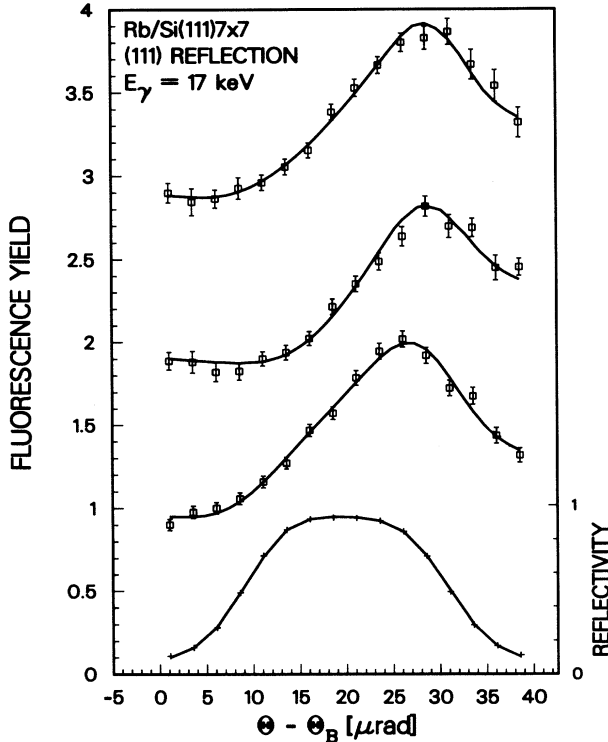


FIG. 2. Rb/Si(111)7×7, (111) reflection at 17 keV energy. Experimental data points and theoretical fits to the data (solid lines, see Sec. III for details), all normalized for the Rb $K\alpha$ fluorescence yield (\square) and substrate reflectivity ($+$) as a function of reflection angle. From bottom to top: reflectivity; Rb fluorescence yield for $\Theta_{\text{Rb}} = 1.00$, 1.02 (vertical offset = 1), and 0.44 ML (vertical offset = 2). For details see Table I.

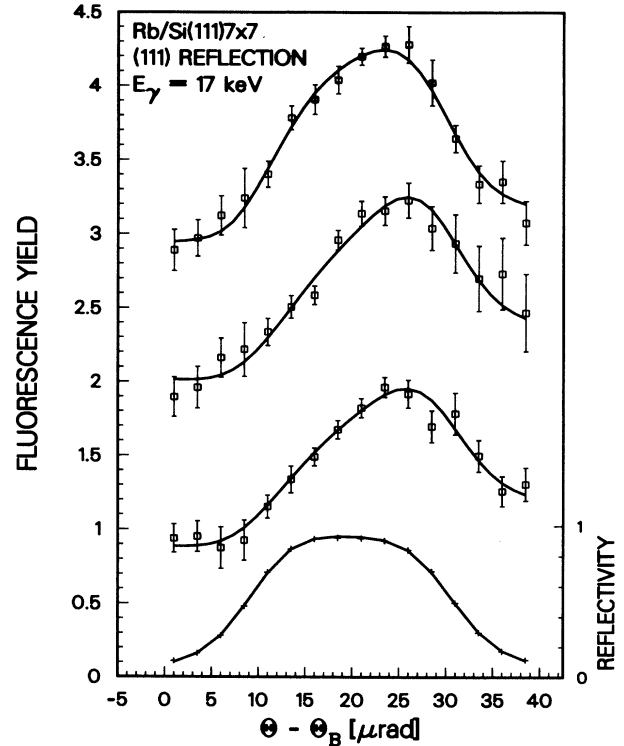


FIG. 3. Rb/Si(111)7×7, (111) reflection at 17 keV energy. Experimental data points and theoretical fits to the data (solid lines, see Sec. III for details), all normalized for the Rb $K\alpha$ fluorescence yield (\square) and substrate reflectivity ($+$) as a function of reflection angle. From bottom to top: reflectivity; Rb fluorescence yield for $\Theta_{\text{Rb}} = 0.16$, 0.08 (vertical offset = 1), and 0.08 ML (vertical offset = 2). For details see Table I.

tern weakened and only the first order spots could be seen at saturation. A mild annealing (up to 400–500 °C) produced a redistribution of the intensity, but we were not able to observe the 1×3 reconstruction,^{5,12} in agreement with Tikhov, Surnev, and Kiskinova,¹³ who reported its appearance only when evaporating at a temperature of ~500 °C (for Na). Annealing to higher temperatures (500–600 °C) produced the reappearance of the 7×7 pattern, but only the first order spots and the seventh order spots closer to them could be seen.

V. DISCUSSION

Since the LEED patterns reveal that a 7×7-like symmetry remained most of the time, and in view of the STM results,^{10,11} we will consider the adsorption sites of the 7×7 and the 1×1 surfaces. The atomic geometry of the Si(111)7×7 reconstruction (shown in Fig. 1) corresponds to the well known dimer-adatom-stacking fault model by Takayanagi *et al.*²⁸ The on-top site (on top of the dangling bond of one bulklike Si atom) is labeled *A*; the 3F-normal-hollow site *B* (also called “open” or *H*₃); the 3F eclipsed site *B*_{*e*} (also called “filled” or *T*₄); and the adatom on-top site (on top of the dangling bond of

a Si adatom) *C*. These sites are shown in Fig. 1, and are also possible on the 1×1 surface (excluding site *C*). Note that sites *A* and *B* present different distances to the [220] plane depending on whether they correspond to the faulted or to the unfaulted half of the 7×7 unit cell. This difference would not be observed, of course, in the case of a 1×1 surface.²² It affects the value of the (220) phase and fraction, provided that both halves are occupied. We do not consider other sites at the 7×7 surface (large hollows, bridge on the dimers, etc.) since they represent a smaller percentage of the surface and furthermore there is no reported preferential adsorption of metals on these sites.

The expected value of the phase (Φ_j) for occupation of a certain site depends on the alkali-metal/silicon bond length. There is a considerable variation in the theoretically calculated bond lengths in the case of alkali metals on silicon surfaces, ranging from values corresponding to an ionic type of bonding^{29–31} to a covalent type.^{2,17,21,32} Experimental values have been obtained by means of surface-extended x-ray-absorption fine structure (SEXAFS) for some interfaces, showing in all cases bond lengths equal, to a very good approximation to the sum of covalent radii of the alkali metal and sili-

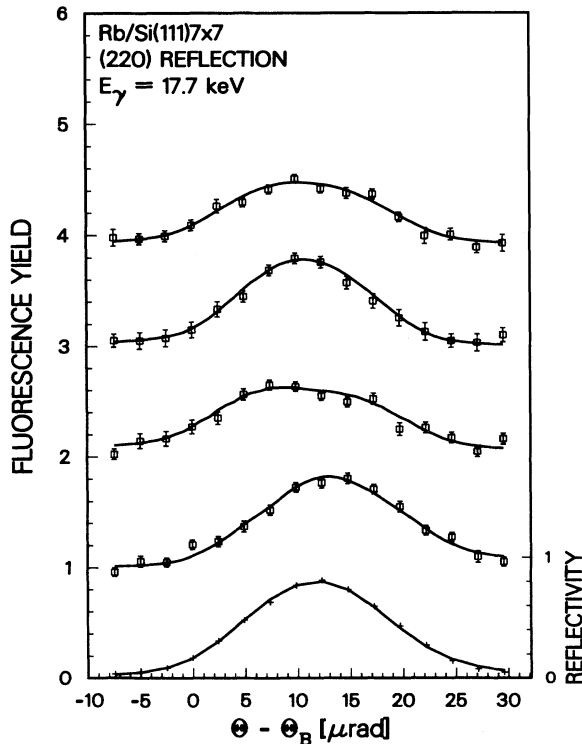


FIG. 4. Rb/Si(111)7×7, (220) reflection at 17.7 keV energy. Experimental data points and theoretical fits to the data (solid lines, see Sec. III for details), all normalized for the Rb $K\alpha$ fluorescence yield (\square) and substrate reflectivity ($+$) as a function of reflection angle. From bottom to top: reflectivity; Rb fluorescence yield for $\Theta_{\text{Rb}} = 1.16$, 0.44 (vertical offset = 1), 0.36 (vertical offset = 2), and 0.34 ML (vertical offset = 3). For details see Table I.

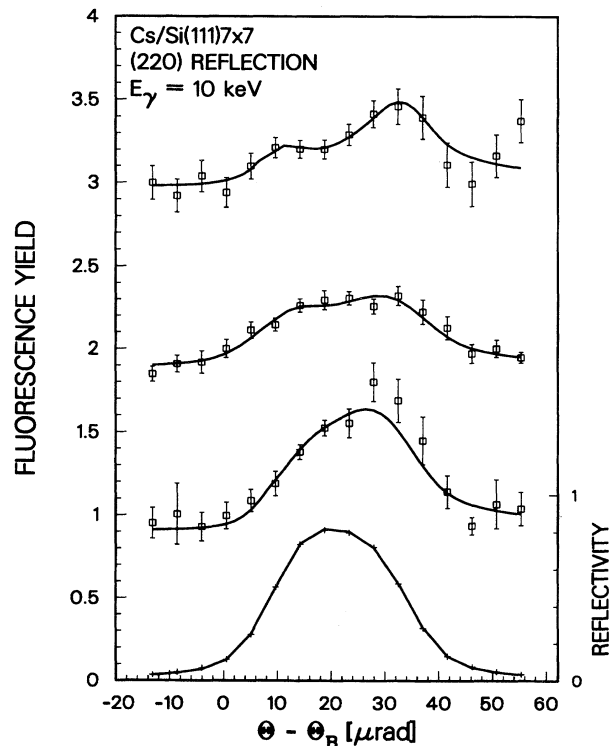


FIG. 5. Cs/Si(111)7×7, (220) reflection at 10 keV energy. Experimental data points and theoretical fits to the data (solid lines, see Sec. III for details), all normalized for the Rb $K\alpha$ fluorescence yield (\square) and substrate reflectivity ($+$) as a function of reflection angle. From bottom to top: reflectivity; Rb fluorescence yield for $\Theta_{\text{Cs}} = 0.48$, 0.28 (vertical offset = 1), and 0.10 ML (vertical offset = 2). For details see Table II.

TABLE I. Experimental results for Rb/Si(111)7×7 and estimated percentages of Rb atoms at each site (assuming $\sum f_j \geq 0.8$; see text for details). The error bars in the percentages denote the acceptable range of values for the corresponding $\Phi_{(hkl)}$ and $f_{c,(hkl)}$. Occupation of both the faulted (/f) and unfaulted (/u) halves of the unit cell was taken into account. Data with a very low f_c have not been fitted. The number in parentheses after each value indicates the error bar in the last figure [e.g., $0.98(2) = 0.98 \pm 0.02$]. Two (220) data (where no exposure time appears) were obtained with the surface held at fixed temperature during the evaporation.

(111) reflection						
Treatment	RT	15 s 100 °C	15 s 350 °C	15 s 420 °C	15 s 420 °C	180 s 420 °C
Φ^a	0.98(2)	0.90(2)	0.94(2)	1.03(3)	1.04(3)	1.15(3)
f_c^b	0.38(2)	0.56(2)	0.46(2)	0.37(4)	0.38(4)	0.45(7)
Θ^c	1.00	1.02	0.44	0.16	0.08	0.08
B, B_e (%)	50 ± 10	70 ± 10	60 ± 10	40 ± 10	40 ± 10	25 ± 10
A (%)	15 ± 10	10 ± 10	15 ± 15	37 ± 5	37 ± 5	45 ± 10
C (%)	17 ± 5	15 ± 10	15 ± 10	15 ± 10	15 ± 10	15 ± 10
(220) reflection						
Treatment	RT	at 350 °C	15 s 350 °C	15 s 400 °C	15 s 420 °C	at 350 °C
Φ^a	1.06(4)	0.91(4)	0.71(2)	1.39(8)	0.69(6)	0.19(3)
f_c^b	0.12(2)	0.18(4)	0.16(2)	0.08(3)	0.07(3)	0.14(4)
Θ^c	1.16	0.67	0.44	0.36	0.34	0.25
$A/u, B_e$ (%)	25 ± 5	15 ± 5	25 ± 5			35 ± 5
$A/f, C, B/f$ (%)	40 ± 5	35 ± 5	25 ± 5			35 ± 10
B/u (%)	30 ± 5	35 ± 10	37 ± 5			20 ± 5

^a Φ , phase.

^b f_c , coherent fraction.

^c Θ , coverage (ML±10%).

con [K/Si(100),³³ Na/Si(100),³⁴ Cs/Si(111) (Ref. 35)]. Following this evidence, and considering also the values provided by semiempirical models,^{36,37} we have assumed a covalent type of bonding, with bond lengths given by the sum of covalent radii (3.33 ± 0.10 Å for Rb-Si and 3.52 ± 0.10 Å for Cs-Si). The error bars of these values take into account both possible inaccuracies derived from this simplistic image, and bond-length changes correlated with the detailed geometry of the adsorption site.³⁶ Tables III and IV present the expected values of the phases [(111) and (220)] for occupation of sites A, B, B_e , and C .

The experimental data show that the coherent phases

TABLE II. Experimental results for Cs/Si(111)7×7 [(220) reflection] and estimated percentages of Cs atoms at each site (assuming $\sum f_j \geq 0.8$; see text for details). The error bars in the percentages denote the acceptable range of values for the corresponding $\Phi_{(220)}$ and $f_{c,(220)}$. Occupation of both the faulted (/f) and unfaulted (/u) halves of the unit cell was taken into account.

Treatment	RT	90 s 450 °C	40 s 500 °C
Φ^a	0.97(4)	0.81(2)	0.83(3)
f_c^b	0.17(2)	0.23(3)	0.34(3)
Θ^c	0.48	0.28	0.10
$A/u, B_e$ (%)	19 ± 5	23 ± 10	18 ± 10
$A/f, C, B/f$ (%)	35 ± 10	22 ± 10	21 ± 10
B/u (%)	37 ± 10	45 ± 5	51 ± 5

^a Φ , phase.

^b f_c , coherent fraction.

^c Θ , coverage (ML±10%).

follow similar trends for both alkali metals. These trends can be correlated with the observed ranges of LEED patterns. The general behavior is as follows: at RT certain values of $\Phi_{(111)}$ and $\Phi_{(220)}$ are obtained (1×1 LEED pattern). After a moderate annealing, both values change and are stabilized within a temperature range of ~100–150 °C (redistribution of intensity within the 1×1 LEED pattern). After annealing to higher temperatures and further coverage reduction, $\Phi_{(111)}$ significantly increases in both cases (reappearance of 7×7 spots). At these coverages (< 0.15 ML) the intensity of fluorescence lines was so low that almost no (220) measurement could be performed. We note that the values of the (111) coherent phases in the case of Rb are always smaller than for Cs (see also Ref. 15). In particular, in the case of the (111) reflection (distance perpendicular to the surface), the values are about 10% smaller, in good agreement with the

TABLE III. Expected phases $\Phi_{(111)}$ and $\Phi_{(220)}$ for Rb/Si(111)7×7 and the considered sites (bond length 3.33 ± 0.10 Å).

Site	$\Phi_{(111)}$	$\Phi_{(220)}$	
		Unfaulted	Faulted
A^a	1.19(3)	1.42(5)	1.08(5)
B^b	0.92(5)	0.72(6)	1.06(6)
B_e^c	0.92(5)	1.39(6)	1.39(6)
C^d	1.44(3)	1.08(5)	1.08(5)

^a A , on-top site.

^b B , threefold-hollow site (normal).

^c B_e , threefold-hollow site (eclipsed).

^d C , adatom on-top site.

TABLE IV. Expected phases $\Phi_{(111)}$ and $\Phi_{(220)}$ for Cs/Si(111)7×7 and the considered sites (bond length 3.52 ± 0.10 Å).

Site	$\Phi_{(111)}$	$\Phi_{(220)}$	
		Unfaulted	Faulted
A^a	1.24(3)	1.49(5)	1.16(5)
B^b	0.99(4)	0.82(6)	1.16(6)
B_e^c	0.99(4)	1.49(6)	1.49(6)
C^d	1.49(3)	1.16(5)	1.16(5)

^a A , on-top site.

^b B , threefold-hollow site (normal).

^c B_e , threefold-hollow site (eclipsed).

^d C , adatom on-top site.

difference expected from the respective atomic sizes of Cs and Rb and the occupied adsorption site (see below). To determine the adsorption site we have considered models of two and three types of sites (including A -, B -, B_e -, and C -type sites). The estimated fraction f_j of atoms at each site depends on the assumed model (bond length, degree of order, number of coherent sites, surface relaxation, etc.). The fractions obtained for a Rb-Si bond length of (3.3 ± 0.1) Å appear in Table I, together with the experimental values. The same information is included in Table II for Cs. In the case of (220) reflection, sites that correspond to the same (or very close) position have been grouped together. The presence of several sites for a certain position makes it difficult to discriminate between them.

In view of the three ranges observed (high coverage, nonannealed; high to intermediate coverages, annealed; low coverages, annealed), we will analyze separately the results of each range (see Tables I and II). In the case of Cs [see Table II for the (220) data], the results of the fit are very similar, and this applies for all the coverages studied, the main difference being that the occupation of A and C sites is smaller by a factor 1–2 as compared to the Rb case.

A. Saturation coverage

The Rb-Si bond length was varied from 3.1 up to 3.5 Å, but no significant changes were observed in the occupation of the different sites, indicating that a change in the bonding distance has no drastic effect on our conclusions. The degree of order and the number of sites are more important parameters. If the C sites are not occupied, then the fraction of coherently located atoms f_0 (the commensurate factor, $f_0 = \sum_{j=1}^n f_j$) is below 0.7 (see Ref. 15). When the C sites are included, f_0 increases up to one when about 25% of the atoms are at the C site. In Table I are included all those combinations of f_j which give a value of $f_0 \geq 0.8$. Note that the fractions f_j are coupled and that not every possible combination agrees with the experimental data. The conclusion of the results in the case of saturation is that several adsorption sites coexist, the hollow sites (B , B_e) being more occupied than the on-top sites (A and C).

B. Intermediate coverage

As the coverage decreases upon mild annealing in the temperature range of 450–500 °C (for Cs) and 300–350 °C (for Rb), the adsorption on the hollow site is promoted. In both cases a good agreement with the expected (111) and (220) phases for the B -type site at the unfaulted parts is obtained (about 0.90 and 0.70, respectively). Daimon and Ino,⁵ Tikhov, Surnev, and Kisinova,¹³ and Jeon *et al.*¹⁴ observed a 1×3 reconstruction of the alkali metal overlayer when evaporating the alkali-metal on a surface held at high temperature. Possible reasons could be that the adatom removal is facilitated at elevated temperatures, or an important role of kinetic limitations associated with alkali-alkali interaction. In any case the formation of 1×3 alkali-metal domains is a thermally activated process which only takes place efficiently at elevated temperatures. Under these circumstances, one would obtain 1×3 domains large enough to observe the LEED pattern only when evaporating at high temperature,¹³ but this would not exclude the formation of smaller domains after annealing a layer deposited at RT. In fact, STM results by Hashizume and co-workers^{10,11} show the existence of such domains for annealed interfaces, i.e., under preparation conditions which would not produce a 1×3 LEED pattern. We propose that our observation of the B site in this temperature range is related to the formation of similar 1×3 domains. This assignment also explains why unfaulted sites are predominant, since there is no faulting at the 1×3 reconstruction.^{10,11} The size of the 1×3 domains is expected to be small (i.e., not enough to produce a 1×3 LEED pattern), and evaporation at high temperature would be needed to get large-sized 1×3 patches. The relatively low value of $f_{c,(220)}$ could be related to a possible incommensurate nature of the 1×3 reconstruction,^{10,11} associated with the presence of three 1×3 domains,¹³ or to partial occupation of other type of sites (B_e , B at faulted parts, etc.). Since we do not know the size of the 1×3 patches present at our surfaces (the mismatch with the substrate would be significant only for large-sized patches), we can only speculate, but the relatively high $f_{c,(111)}$ favors the second possibility, which is reflected in the data of Table I: after a mild annealing, the occupation of B , B_e sites reaches a maximum. Further annealing promotes the occupation of A sites (see next), while C sites present an approximately constant occupation. This behavior is compatible with the percentages obtained from the (220) measurements. In addition, in one case the value of $\Phi_{(220)}$ differs from the others (0.39 vs 0.70; see Table I), and is very similar to the expected value for B_e sites. Since the coherent fraction of this experiment was very low (0.08), it is not possible to extract definitive conclusions from the result, but it could well be that the energy difference between B and B_e sites is not very large,^{17,19,20} and small differences in the preparation conditions could favor the occupation of B_e over B type of sites. In fact, in the case of Rb the results of the (220) reflection display a substantially smaller coherent fraction than in the case of Cs, which is probably an

indication of a worse ordering of Rb atoms compared to Cs atoms.⁹

C. Low coverage

The third range observed appears at very low coverages, when a significant increase in $\Phi_{(111)}$ is detected, for both Rb and Cs. Unfortunately, due to the low counting rate almost no (220) measurement could be performed to completely clarify the origin of the observed increase. In addition, there is a concomitant increase of $f_{c,(111)}$. In the case of Rb, $f_{c,(111)}$ increases up to 0.45, while for Cs it reaches a value of 0.71.¹⁵ Such a significant increase usually means that an improvement of the adsorbate ordering is taking place, and that one type of adsorption site is favored over the other types. The observed change in position ($\Delta\Phi_{(111)} \simeq 0.25$ or 0.8 Å for Rb, and $\Delta\Phi_{(111)} \simeq 0.10$ or 0.3 Å for Cs) should be then attributed to a change in the adsorption distance to the surface. Several possibilities could, in principle, explain such change: (a) a change of adsorption site, keeping the same bond length; (b) a change of bond length to a longer value, keeping the same adsorption site; (c) a simultaneous change of adsorption site and bond length.

Since the change of $\Phi_{(111)}$ is observed for an annealed overlayer (i.e., well ordered), in principle the adsorption site should not be modified. In the case of alkali-metal/silicon interfaces however, there is a number of studies where coverage-dependent adsorption-site changes have been reported.⁹ These changes are due to a significant coverage dependence of the alkali-alkali interaction, and thus they cannot be excluded. Moreover, due to the structure of the 7×7 reconstruction (formed basically by ordered dimers and adatoms) a high annealing temperature could be needed for the occupation of certain adsorption sites, e.g., those which involve a modification of the 7×7 reconstruction with Si-Si bond breaking and adatoms displacing.³⁸ In our case, an increase in the (111) position is detected. This observation is consistent with occupation of *C*- or *A*-type sites after annealing. Our results favor that *A*-type sites are occupied under these conditions on the following basis: the result of a three-position fit to the data indicates this behavior (see Table I) from both $\Phi_{(111)}$ and $\Phi_{(220)}$ values [in particular for the (220) Rb measurement taken at 0.25 ML]; the value of the final $\Phi_{(111)}$ fits quite well with the expected value for the *A* site, never exceeding it, as one would expect in the case of occupation of *C* sites.

The second possibility of explaining the observed increase in $\Phi_{(111)}$ is a coverage-dependent bond-length change. As we showed in a previous publication,¹⁵ it has been proposed that the alkali-metal/silicon interaction changes from predominantly ionic at low coverages to covalent at higher coverages,³⁹⁻⁴¹ i.e., a behavior like the one initially proposed by Gurney in the case of metallic substrates.⁴² This change would be concomitant with the conspicuous work function decrease observed for all alkali-metal/silicon interfaces.¹ Assuming that the adsorption site is of *B* type at intermediate coverages, the observed increase in position would mean a

large increase in bond length, 0.8 Å. The observation of a significant occupation of alkali-metal *s* levels at very low coverages,⁴³ the bond-length values determined by SEXAFS,^{33,34} and recent photoemission results,⁴⁴ do not favor theoretical models predicting coverage-dependent bond-length changes.⁴⁵ On the contrary, calculations by Ishida and Terakura⁴⁶ and by Kobayashi *et al.*² present a picture [for K/Si(100) 2×1] in agreement with experiments, where the charge transfer would be fractional and rather small at all coverages and a weak covalent bonding explains the strong work function reduction by a polarization dependent interaction. These considerations imply a bond length only slightly dependent on coverage. On the other hand, Batchelor and King³⁵ have reported an increase in bond length of 0.3 ± 0.1 Å when going from 1.0 ML to 0.4 ML in the case of Cs/Si(111) 7×7 . However, their analysis has been questioned by other authors^{47,48} in the case of an analogous system where a similar behavior was observed.⁴⁹

We have finally considered the possibility of a simultaneous change of adsorption site and bond length. In this case, either occupation of *A* sites or occupation of *C* sites should occur, the latter with a bond length shorter than the sum of covalent radii, to explain the experiments. Even in this case, the expected $\Phi_{(111)}$ values for *C* occupation are too large for reasonable values of the bond length. On the basis of our data we cannot determine whether the bond length remains constant or not, but a change significant enough to account for the increase of $\Phi_{(111)}$ can be discarded. Furthermore, from the experiments on Rb/Si(111) 7×7 it is clear that a longer anneal at the same temperature changes the position without altering the coverage [see the last two (111) measurements in Table I]. On the contrary, all models which predict a change in bond length associate this process with a change of coverage.

On the other hand, the main obstacle to reaching definitive conclusions is the fact that too many different positions are present in (220) data, due to the existence of a stacking fault in one-half of the 7×7 unit cell. In order to overcome this difficulty, we have performed a similar study on Rb/Si(211) 2×1 . The Si(211) surface is composed of narrow (two-unit cells) (111) terraces separated by (100) steps. It presents no stacking fault. The results of this study (using three independent Bragg reflections) have been presented elsewhere.⁵⁰ They can be summarized as follows: at saturation coverage, mainly *B_e* sites are occupied, but as the coverage diminishes, *A* sites are predominant. Assuming no surface relaxation,²¹ a limit of 0.2 ± 0.2 Å was set for a possible Rb-Si bond length change. In view of the similarity of the surface, these results support an analogous behavior also with Si(111). Therefore, we conclude that our results with Si(111) are basically explained by a change of position (and not a change in bond length). We note that a direct comparison of this limit with the value of Batchelor and King³⁵ is difficult, in view of the different adsorption geometry proposed in their model. Hashizume co-workers^{10,11} proposed occupation of *C* sites for RT-deposited low alkali-metal coverages ($\Theta < 0.07$ ML) on the basis of the observation by STM of dark regions at *C* adsorption sites.

Our data do not discard this possibility, but point to predominant occupation of *A* sites at low coverages, which could be due to the fact that in our case the surface had been annealed to elevated temperatures, or to difficulties in identifying the adsorption sites at very low coverages by STM due to the influence of other factors (e.g., residual gas adsorption, electronic effects, etc.). As a final conclusion, we propose that *A*-type sites are occupied at low coverages, since this model best describes the experimental phases and fractions for this coverage range, as well as evidence for other surfaces of similar symmetry.

Very recently, an XSW study of Rb and Cs/Si(111)7×7 by Lagomarsino *et al.*¹⁶ has appeared. Their conclusions are to some extent different from ours. In particular, they did not observe any significant coverage dependence of the adsorption site, which is probably due to the lack of annealing in their case. Thus, they found a mixture of *B*, *B_e*, and *A* sites, similar to the situation observed at RT in our case.

VI. CONCLUSIONS

The adsorption of alkali metals (Cs,Rb) on Si(111)7×7 has been studied by x-ray standing wave. The conclu-

sions can be summarized as follows: both adsorbates behave in a similar way, characterized by a rather disordered adsorption at room temperature [with presence of on-top, 3F-hollow sites of normal (*B*) and eclipsed-type (*B_e*), and probably adatom on top sites]. After annealing to 450–500 °C (in the case of Cs) or 300–350 °C (in the case of Rb), a much better ordered adlayer was obtained. We relate this range to the 1×3 phase observed by other authors. The adsorption site is of *B* type in this case. After annealing to higher temperatures a significant increase in the adsorbate-substrate distance was detected. Several possibilities could explain this change, but the collected experimental evidence favors occupation of on-top sites at these very low coverages.

ACKNOWLEDGMENTS

This work was partially financed by the German Ministry for Science and Technology. V.E. thanks the Academy of Finland and the Finnish Cultural Foundation, and E.G.M. thanks the Alexander von Humboldt Foundation for financial support.

* Permanent address: Department of Physics, University of Helsinki, 00014 Helsinki, Finland.

† Permanent address: Departamento de Física de la Materia Condensada C-III, Universidad Autónoma de Madrid, 28049 Madrid, Spain.

¹ See, for example, *Metallization and Metal-Semiconductor Interfaces*, edited by I.P. Batra (Plenum, New York, 1988).

² K. Kobayashi, Y. Morikawa, K. Terakura, and S. Blügel, *Phys. Rev. B* **45**, 3469 (1992).

³ I.P. Batra, *Phys. Rev. B* **43**, 12322 (1991), and references therein.

⁴ I.P. Batra, *J. Vac. Sci. Technol. A* **8**, 3425 (1990), and references therein.

⁵ H. Daimon and S. Ino, *Surf. Sci.* **164**, 320 (1985).

⁶ S. Mizuno and A. Ichimiya, *Appl. Surf. Sci.* **33/34**, 38 (1988).

⁷ K.O. Magnusson and B. Reihl, *Phys. Rev. B* **41**, 12071 (1990).

⁸ K.O. Magnusson, S. Wiklund, R. Dudde, and B. Reihl, *Phys. Rev. B* **44**, 5657 (1991).

⁹ B. Reihl, R. Dudde, L.S.O. Johanson, K.O. Magnusson, S.L. Sorensen, and S. Wiklund, *Appl. Surf. Sci.* **56–58**, 123 (1992).

¹⁰ T. Hashizume, Y. Hasegawa, I. Sumita, and T. Sakurai, *Surf. Sci.* **246**, 189 (1991).

¹¹ T. Hashizume, K. Motai, Y. Hasegawa, I. Sumita, H. Tanaka, S. Amano, S. Hyodo, and T. Sakurai, *J. Vac. Sci. Technol. B* **9**, 745 (1991).

¹² W.C. Fan and A. Ignatiev, *Phys. Rev. B* **41**, 3592 (1990).

¹³ M. Tikhov, L. Surnev, and M. Kiskinova, *Phys. Rev. B* **44**, 3222 (1991).

¹⁴ D. Jeon, T. Hashizume, T. Sakurai, and R.F. Willis, *Phys. Rev. Lett.* **69**, 1419 (1992).

¹⁵ V. Eteläniemi, E.G. Michel, and G. Materlik, *Phys. Rev. B* **44**, 4036 (1991).

¹⁶ S. Lagomarsino, F. Scarinci, P. Castrucci, C. Gianini, E.

Fontes, and J.R. Patel, *Phys. Rev. B* **46**, 13631 (1992).

¹⁷ J.E. Northrup, *J. Vac. Sci. Technol. A* **4**, 1404 (1986).

¹⁸ I.P. Batra and S. Ciraci, *Phys. Rev. B* **37**, 8432 (1988).

¹⁹ S. Ossicini, C. Arcangeli, and O. Bisi, *Phys. Rev. B* **42**, 7671 (1990).

²⁰ F. Huaxiang and Y. Ling, *Surf. Sci.* **250**, L373 (1991).

²¹ I. Moullet, W. Andreoni, and M. Parrinello, *Surf. Sci.* **269/270**, 1000 (1992).

²² E.G. Michel, Th. Pauly, V. Eteläniemi, and G. Materlik, *Surf. Sci.* **241**, 111 (1991).

²³ A. Ishizaka and Y. Shiraki, *J. Electrochem. Soc.* **133**, 666 (1986).

²⁴ P. Funke and G. Materlik, *Surf. Sci.* **188**, 378 (1987).

²⁵ J. Zegenhagen, G. Materlik, and W. Uelhoff, *J. X-ray Sci. Technol.* **2**, 214 (1990), and references therein.

²⁶ B.W. Batterman and H. Cole, *Rev. Mod. Phys.* **36**, 681 (1964).

²⁷ P.L. Cowan, J.A. Golovchenko, and M.F. Robins, *Phys. Rev. Lett.* **44**, 1680 (1980).

²⁸ K. Takayanagi, Y. Tanishiro, M. Takahashi, and S. Takahashi, *J. Vac. Sci. Technol. A* **3**, 1502 (1985).

²⁹ S. Ciraci and I.P. Batra, *Phys. Rev. Lett.* **58**, 1982 (1987).

³⁰ S. Ciraci and I.P. Batra, *Phys. Rev. B* **37**, 2955 (1988).

³¹ R. Ramirez, *Phys. Rev. B* **40**, 3962 (1989).

³² Y. Ling, A.J. Freeman, and B. Delley, *Phys. Rev. B* **39**, 10144 (1989).

³³ T. Kendelewicz, P. Soukiassian, R.S. List, J.C. Woicik, P. Pianetta, I. Lindau, and W.E. Spicer, *Phys. Rev. B* **37**, 7115 (1988).

³⁴ S.T. Kim, P. Soukiassian, L. Barbier, S. Kapoor, and Z. Hurych, *Phys. Rev. B* **44**, 5622 (1991).

³⁵ D.R. Batchelor and D.A. King, *Chem. Phys. Lett.* **186**, 19 (1991).

³⁶ K.A.R. Mitchell, *Surf. Sci.* **149**, 93 (1985).

³⁷ P.H. Citrin, *Surf. Sci.* **184**, 109 (1987).

³⁸ J.J. Boland and J.J. Villarrubia, *Phys. Rev. B* **41**, 9865

- (1990).
- ³⁹ T. Kato, K. Ohtomi, and M. Nakayama, *Surf. Sci.* **209**, 131 (1989), and references therein.
- ⁴⁰ H. Tochihara, M. Kubota, M. Miyo, and Y. Murata, *Surf. Sci.* **158**, 497 (1985).
- ⁴¹ E.M. Oellig, E.G. Michel, M.C. Asensio, R. Miranda, J.C. Duran, A. Muñoz, and F. Flores, *Europhys. Lett.* **5**, 727 (1988).
- ⁴² R.W. Gurney, *Phys. Rev.* **47**, 479 (1935).
- ⁴³ S. Nishigaki, N. Oishi, S. Matsuda, N. Kawanishi, and T. Sasaki, *Phys. Rev. B* **39**, 8048 (1989).
- ⁴⁴ D. Lin, T. Miller, and T.C. Chiang, *Phys. Rev. B* **44**, 10 719 (1991).
- ⁴⁵ S. Ciraci and I.P. Batra, *Phys. Rev. Lett.* **56**, 877 (1986).
- ⁴⁶ H. Ishida and K. Terakura, *Phys. Rev. B* **40**, 11 519 (1989).
- ⁴⁷ M. Kerkar, D. Fisher, D.P. Woodruff, R.G. Jones, R.D. Diehl, and B. Comie, *Phys. Rev. Lett.* **68**, 3204 (1992).
- ⁴⁸ D.M. Riffe, G.K. Wertheim, and P.H. Citrin, *Phys. Rev. Lett.* **64**, 571 (1990).
- ⁴⁹ G.M. Lamble, R.S. Brooks, D.A. King, and D. Norman, *Phys. Rev. Lett.* **61**, 1112 (1988).
- ⁵⁰ E.G. Michel, V. Eteläniemi, and G. Materlik, *J. Vac. Sci. Technol.* (to be published).